

DUALITY IN $\pi^- + p \rightarrow \pi^+ + \Delta^-$ AT 1.5-1.8 GeV

A. Kernan*

University of California, Riverside, California 92502

and

Harvey K. Shepard†

University of California, Riverside, California 92502, and
University of New Hampshire, Durham, New Hampshire 03824‡

(Received 16 October 1969)

Considerable evidence for duality is found in a study of the amplitude for $\pi^- p \rightarrow \pi^+ \Delta^-$ scattering at center of mass energies 1.5-1.8 GeV. Cancellation between dominant contributions from the $\frac{5}{2}^+$, $F_{15}(1690)$ and the $\frac{3}{2}^-$, $D_{13}(1520)$ is primarily responsible for the local averaging.

We have examined the four independent amplitudes constructed from experiment¹ for the reaction $\pi^- + p \rightarrow \pi^+ + \Delta^-$ and find considerable evidence in support of the hypothesis of local averaging in the low intermediate energy region.

Assuming that no significant $I=2$ exotic $\pi\pi$ resonances exist, the duality hypothesis² implies in the present case that each appropriately constructed t -channel amplitude will have an imaginary part which averages "locally" to zero. For a range of physical t values, $-0.3 \leq t \leq -0.011$, in the rather narrow energy interval, 1.5 GeV $\leq E_{\text{cm}} \leq 1.76$ GeV, we find strong duality shaping in each of the four helicity amplitudes, especially at low momentum transfer. Generally speaking, we find that good d -shaping results from the cancellation of contributions from the two nucleon resonances $F_{15}(1690)$ and $D_{13}(1520)$ and a concomitant small $D_{15}(1690)$ and background contri-

bution.

The s -channel helicity amplitudes for $\pi^- + p \rightarrow \pi^+ + \Delta^-$ were constructed from the preliminary partial-wave analysis of the Stanford Linear Accelerator Center-Lawrence Radiation Laboratory (SLAC-LRL) inelastic pion-nucleon experiment reported at the Vienna Conference.¹ We shall present results based on their resonance-plus-background solution shown in Table I.³ Of special interest in Table I are (1) the dominance of the three nucleon states with no resonant $I=\frac{3}{2}$ partial waves being necessary; and (2) the negative sign of $[\chi_{\pi N}(D3)\chi_{\pi\Delta}(S3)]^{1/2}$.⁴ Such a negative sign, which is also the sign of the imaginary part of the corresponding partial-wave amplitude, cannot appear in an elastic amplitude.

The four independent s -channel helicity amplitudes are formed by summing the phenomenological partial-wave amplitudes of Table I:

$$f_{\mu_0, \lambda_0}^S(s, t) = (s/p_{\pi N} p_{\pi\Delta})^{1/2} \sum_{J, L, L', I} (2L+1)^{1/2} (2L'+1)^{1/2} C(L\frac{1}{2}J; 0\lambda) C(L'\frac{3}{2}J; 0\mu) d_{\lambda\mu}^J(\cos\theta_s) T_{L'L}^{J, I}(s), \quad (1)$$

where L, λ (L', μ) refer to the orbital angular momentum and helicity of the initial (final) state.⁵ The resonant partial-wave amplitudes are normalized as follows:

$$T_{L', L}^{J, I} = [\chi_{\pi N}(L)\chi_{\pi\Delta}(L')]^{1/2} / (\epsilon - i),$$

where

$$\epsilon = (E_{\text{res}} - E_{\text{cm}}) / (\Gamma/2). \quad (2)$$

The t -channel helicity amplitudes $f_{\mu'\lambda', 00}^t$ are then obtained from $f_{\mu, \lambda}^s$ by direct application of the Trueman-Wick helicity crossing relations,⁶⁻⁸

$$f_{\mu'\lambda', 00}^t(s, t) = \sum_{\lambda, \mu} d_{\lambda'\lambda}^{1/2}(X_N) d_{\mu'\mu}^{3/2}(X_\Delta) f_{\mu, \lambda}^s(s, t). \quad (3)$$

Finally we form the kinematic-singularity-free amplitudes,⁸ $\tilde{f}_{\mu'\lambda', 00}^t(s, t)$. We have

$$\tilde{f}_{\mu'\lambda', 00}^t = T_N T_p^2(\Phi)^{-1/2} |\lambda' - \mu'| f_{\mu'\lambda', 00}^t.$$

Under $s \leftrightarrow u$ ($\nu \leftrightarrow -\nu$),⁹

$$\tilde{f}_{\lambda_1 \lambda_2, 00}^{t, (I)}(-\nu) = (-1)^{I + |\lambda_1 - \lambda_2|} \tilde{f}_{\lambda_1 \lambda_2, 00}^{t, (I)}(+\nu).$$

The isospin crossing relation is

$$f(I_t = 2) = f^S(p\pi^- \rightarrow \Delta^- \pi^+) = (\frac{1}{3})^{1/2} f(I_s = \frac{1}{2}) - (2/15)^{1/2} f(I_s = \frac{3}{2}) = -(s \leftrightarrow u).$$

In our case, assuming there is no significant $I = 2$ $\pi\pi \rightarrow \bar{N}\Delta$ Regge amplitude, the finite-energy sum rules all have the form

$$\int_{\nu_0}^N \nu^n \text{Im} \tilde{f}_{\mu' \lambda'}^{t(2)}(\nu) d\nu \sim 0. \quad (4)$$

Duality is the hypothesis that the integrand, and hence $\text{Im} \tilde{f}_{\mu' \lambda'}^t$, will itself locally average to zero. The significant question is of course how local is the averaging, that is, how far around any specified energy one must average and how low in energy one can go.

In Fig. 1 we show the imaginary part of each amplitude, $\text{Im} \tilde{f}^t$, for four (physical) values of the momentum transfer (the value $-t = 0.011$ is the minimum momentum transfer at $E_{\text{cm}} = 1500$ MeV). Some prominent features of these curves are the following: (A) All of the amplitudes show strong duality shaping for small $-t$ with generally poorer d shaping as $|t|$ increases. (B) For the strongly d -shaped amplitudes, the "wavelength" of the oscillations around zero is approximately 300-340 MeV¹⁰; i.e., slightly larger than the energy interval of the data, with $\text{Im} \tilde{f}^t$ passing through zero around 1600 MeV. (C) All

Table I. SLAC-LRL partial-wave amplitudes for $\pi^- p \rightarrow \pi^+ \Delta^-$ at cm energies 1.5-1.76 GeV from Ref. 1 (corrected). L (L') is the initial (final) orbital angular momentum. The initial c.m. momentum $p_{\pi N}$ is expressed in GeV.

Resonance amplitudes [see Eq. (2) for normalization]				
$L_2 J(J^P)$	E_{Res} (MeV)	Γ (MeV)	L'	$[\chi_{\pi N}(L) \chi_{\pi \Delta}(L')]^{1/2}$
$F_{15}(\frac{3}{2}^+)$	1690 ± 5	131	P	0.491 ± 0.02
			F	0.035
$D_{15}(\frac{5}{2}^-)$	1680 ± 5	170	D	0.347 ± 0.01
			G	0.020
$D_{13}(\frac{3}{2}^-)$	1520	115	S	-0.374 ± 0.10

Background amplitudes ($T_{L', L}^J, J = a + b \cdot p_{\pi N}$)					
$L_2 J(J^P)$	L'	Rea	Ima	Reb (GeV^{-1})	Imb (GeV^{-1})
$D_3(\frac{3}{2}^-)$	S	-0.08	+0.11	-0.22	-0.15
$P_1(\frac{1}{2}^+)$	P	+0.09	-0.001	+0.03	+0.13
$S_1(\frac{1}{2}^-)$	D	-0.12	+0.08	-0.08	+0.09
$F_7(\frac{7}{2}^+)$	F	-0.013	+0.002	0	0

of the amplitudes show some damping at higher energies. The latter feature is a result of several factors. Probably dominant is the fact that we are moving away from all the resonant peaks. We also expect damping as we go to higher energies, since the range of physical t values is increasing rapidly with $E_{\text{c.m.}}$, whereas the total channel cross section is not.¹ Finally, there is some artificial high-energy damping introduced into the amplitudes when we divide out the kinematical singularities, viz. those contained in the Kibble boundary function⁸ Φ . The damping is greatest for $\tilde{f}_{-3/2, 1/2}^t$ i.e., for the amplitude with the maximum $|\mu' - \lambda'|$.

It should be noted that for the energies and t values shown, the s -channel scattering angle varies over a wide range, from θ_s near zero to almost backward angles.¹¹

In order to see more clearly when and how duality shaping comes about, it is necessary to study (at a specified t) the separate resonance and background contributions to each amplitude.

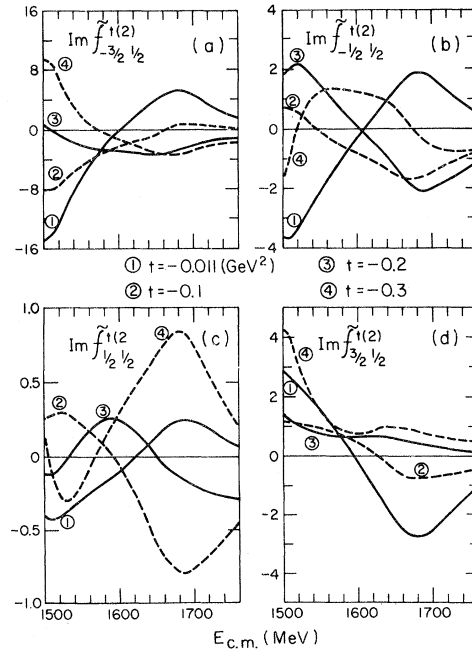


FIG. 1. $\text{Im} \tilde{f}_{\mu' \lambda'}^{t, 00}$ vs $E_{\text{c.m.}}$ for $-t = 0.011, 0.1, 0.2, 0.3$ (GeV^2), corresponding to the curves labeled 1, 2, 3, and 4, respectively.

We illustrate this in Fig. 2 where we have drawn the individual resonance and combined background contributions of Table I to the two amplitudes $(-\frac{1}{2}\frac{1}{2})$ and $(\frac{1}{2}\frac{1}{2})$ for $-t=0.011$ and 0.1 .

From Fig. 2 and the similar curves for the other amplitudes and t values we can observe the following: Strong duality shaping is generally a result of approximately equal and opposite contributions from the $F_{15}(1690)$ and $D_{13}(1520)$ resonances, coupled with a relatively small and flat contribution from the $D_{15}(1680)$ and background amplitudes. This is the typical pattern at small $-t$. In some "good" cases the parts of $\text{Im}\tilde{f}^t$ due to the background and D_{15} are not small, but approximately cancel especially at higher $E_{c.m.}$.

The spacing and peaking of the dominant resonant amplitudes is directly reflected in $\text{Im}\tilde{f}^t$ and accounts both for the wavelength of the oscillations and the vanishing of $\text{Im}\tilde{f}^t$ (roughly halfway between the two peaks) noted above in (B). For small t , the D_{13} generates a somewhat narrower and higher peak at low E than the peak of F_{15} at higher energies.

The cases in which duality fails are not simple to characterize. For most of them, the F_{15} and D_{13} still contribute with opposite signs but now the background and/or D_{15} contribution is large and spoils the cancellation. Typically the combined background contribution is small and flat at low t but becomes larger and develops a low-energy peaking as $-t$ increases.

We have also examined $\text{Im}\tilde{f}^t$ formed from only the resonance contributions in Table I. On the whole this produces little overall change in the degree of duality shaping. We believe that by including the background amplitudes of the (SLAC-LRL) fit our results are less model dependent. Furthermore, one should probably regard the background amplitudes of Table I as mainly representing parts of additional weakly coupled (or unresolved) resonances rather than a true non-resonant background corresponding to some (hitherto undiscovered) $I=2$ Pommeranchuk-like J -plane singularity.¹²

It is clear from the figures that the strength and shape of a resonance contribution to an amplitude depends in a complex way on the t value and helicities, in addition to the resonance parameters and quantum numbers. For example, even the sign of a resonance contribution to a particular t -channel amplitude can change when t is varied by a small amount. Of course, all of this complexity is contained in Eqs. (1) and (3).

Finally, we wish to make several remarks of a

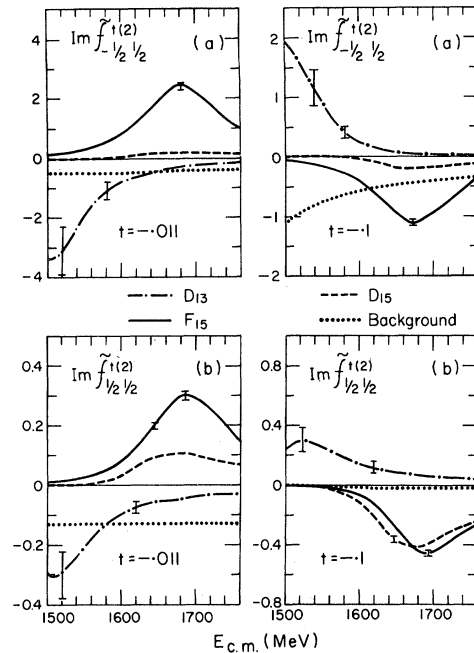


FIG. 2. Individual resonance and total background contributions to (a) $\text{Im}\tilde{f}_{-\frac{1}{2}\frac{1}{2}}^{t(2)}$ and (b) $\text{Im}\tilde{f}_{\frac{1}{2}\frac{1}{2}}^{t(2)}$ for $-t=0.011$ and 0.1 $(\text{GeV})^2$. The error bars indicate the uncertainty in $(\chi_{\pi N \chi_{\pi \Delta}})^{1/2}$ of the resonant amplitudes.

more theoretical nature.

(A) As noted above, in the cases where we have strong d shaping the dominant effect is a cancellation (over a range $\Delta E \approx 320$ MeV) between two nucleon resonances, the $F_{15}(1690)$ and $D_{13}(1520)$. This suggests placing these $\frac{5}{2}^+$ and $\frac{3}{2}^-$ states on exchange-degenerate $N_\alpha-N_\gamma$ Regge trajectories, although the slopes are quite different in the usual nucleon trajectory assignments.¹³

We do not seem to require any further exchange degeneracy between different isospins, as has been suggested in the meson case,¹⁴ to suppress the existence of exotic resonances in the t -channel, i.e., no strong Δ states seem necessary.

Our results are of interest in connection with the recent work of Mandula, Weyers, and Zweig¹⁵ on the consequences of exact and "broken" duality for SU(3), or quark model, baryon trajectories. The exchange degeneracies which they find coming from P - B and P - Δ scattering would be consistent with our suggestion of an exchange degeneracy between the octet $\frac{1}{2}^+$, $\frac{5}{2}^+$ nucleon trajectory and the octet $\frac{3}{2}^-$ trajectory. Their work implies that an exchange degeneracy between the decuplet $\frac{3}{2}^+$ trajectory and the octet $\frac{5}{2}^-$ is also required.

(B) It is interesting to note that we can achieve duality with the F_{15} and D_{13} , two states which satisfy the $(J-L=I-1)$ rule for prominent reso-

nances, discussed by Chiu and Kotanski¹⁶ in their study of "Schmid¹⁷ circles" in pion-nucleon scattering.

(C) The existence of t -channel Regge cuts (with $I=2$) is expected to modify the right-hand side of Eq. (4), especially for large $-t$. However the relative importance of such an extrapolation of cut effects to low s is not clear.

(D) It is worth emphasizing that the sign of an s -channel resonance contribution to a t -channel amplitude depends on many things besides the isospin crossing matrix which has usually been stressed.¹⁸ As Fig. 2 illustrates, the sign also depends on J , L , L' , t , and the inelastic width factor $(\chi_{\pi N} \chi_{\pi \Delta})^{1/2}$.

We are grateful to Dr. A. Brody for several discussions of the SLAC-LRL partial-wave analysis. We also wish to thank Professor B. Desai and Professor G. Zweig for cogent comments.

*Work supported in part by the U. S. Atomic Energy Commission, Contract No. AEC AT(11-1)34P107B.

†Work supported in part by the U. S. Atomic Energy Commission, Contract No. AEC AT(11-1) 34P107A.

‡Present address.

¹A. D. Brody et al., Stanford Linear Accelerator Center Report No. SLAC-PUB 531, 1968 (unpublished), and corrected version.

²R. Dolen, D. Horn, and C. Schmid, Phys. Rev. **166**, 1768 (1968); C. Schmid, Phys. Rev. Letters **20**, 628, 689 (1968).

³The χ^2 for the fit in Table I is 286 for 229 degrees of freedom.

⁴We define $\chi_{\pi N}(L) = \Gamma_{\pi N}(L) / \Gamma_{\text{total}}$, etc.

⁵M. Jacob and G. C. Wick, Ann. Phys. (N.Y.) **7**, 404 (1959). The cross section is $d\sigma/dt = (8\pi S p_{\pi N}^2)^{-1}$

$\times \sum_{\lambda, \mu} |f_{\mu, \lambda}^s|^2$.

⁶T. L. Trueman and G. C. Wick, Ann. Phys. (N.Y.) **26**, 322 (1964); I. Muzinich, J. Math. Phys. **5**, 1481 (1964).

⁷The crossing angles are (using the conventions of Ref. 8) $\cos X_N = [(S+M^2-\mu^2)(t+M^2-M_\Delta^2) + 2M^2(M_\Delta^2-M^2)] \times (S_{\pi N} T_{N\Delta})^{-1}$; $\cos X_\Delta = [-(S+M_\Delta^2-\mu^2)(t+M_\Delta^2-M^2) + 2M_\Delta^2 \times (M_\Delta^2-M^2)] (S_{\pi\Delta} T_{N\Delta})^{-1}$.

⁸L. L. Wang, Phys. Rev. **142**, 1187 (1966), and **153**, 1164 (1967). We define $T_N = [t - (M_\Delta + M)^2]^{1/2}$, $T_D = [t - M_\Delta - M]^2]^{1/2}$, $\Phi = (\frac{1}{2}) [(t - 4\mu^2) T_N^2 T_D^2 - t(S - \mu^2)^2] = (4S)^{-1} (1 - \cos^2 \theta_s) (S_{\pi N} S_{\pi \Delta})^2$, and $S_{\pi \Delta}^2 = [S - (M_\Delta + \mu)^2] [S - (M_\Delta - \mu)^2]$, etc.

⁹This follows from interchanging the two pions; e.g., see F. Gilman and H. Harari, Phys. Rev. **165**, 1803 (1968).

¹⁰The corresponding wavelength in pion-nucleon charge-exchange scattering is more than twice as large. See Ref. 2.

¹¹For example, at 1500 MeV for $t = -0.3$ the value of $\cos \theta_s$ is ~ -0.6 . In general, $\cos \theta_s = (S_{\pi N} S_{\pi \Delta})^{-1} [St + S^2 - S(M_\Delta^2 + M^2 + 2\mu^2) + (M^2 - \mu^2)(M_\Delta^2 - \mu^2)]$.

¹²As mentioned in Ref. 1 the partial-wave fit is not unique with respect to the background amplitudes. In fact a satisfactory solution can also be obtained by replacing the nonresonant amplitudes with the resonances $P_{33}(1730)$, $S_{31}(1634)$, $D_{33}(1679)$, and $P_{11}(1752)$. See A. Donnachie, in Proceedings of the Fourteenth International Conference on High Energy Physics, Vienna, Austria, 1968 (CERN Scientific Information Service, Geneva, Switzerland, 1968). However all solutions contain the three $I = \frac{1}{2}$ resonances of Table I within the quoted errors. (A. D. Brody, private communication).

¹³V. Barger and D. Cline, Phys. Rev. Letters **20**, 298 (1968).

¹⁴H. Lipkin, Nucl. Phys. **B9**, 349 (1969); E. Abers and V. Teplitz, to be published.

¹⁵J. Mandula, J. Weyers, and G. Zweig, Phys. Rev. Letters **23**, 266 (1969); J. Mandula, C. Rebbi, R. Slansky, J. Weyers, and G. Zweig, Phys. Rev. Letters **22**, 1147 (1969). See also R. H. Capps, Phys. Rev. Letters **22**, 215 (1969).

¹⁶C. Chiu and A. Kotanski, Nucl. Phys. **7**, 615 (1968); **8**, 553 (1969).

¹⁷C. Schmid, Phys. Rev. Letters **20**, 628, 689 (1968).

¹⁸See, e.g., H. Harari, in Proceedings of the Fourteenth International Conference on High Energy Physics, Vienna, Austria, September, 1968 (CERN Scientific Information Service, Geneva, Switzerland, 1968).